Research Square

Preprints are preliminary reports that have not undergone peer review.
They should not be considered conclusive, used to inform clinical practice,
or referenced by the media as validated information.

Gene mapping and identification of candidate genes associated with fomesafen herbicide tolerance in Mung bean (Vigna radiata L.)

Huiying Shi
Institute of Cereal and Oil Crops, Hebei Academy of Agriculture and Forestry Sciences
Changyou Liu
Institute of Cereal and Oil Crops, Hebei Academy of Agriculture and Forestry Sciences
Shen Wang
Institute of Cereal and Oil Crops, Hebei Academy of Agriculture and Forestry Sciences
Yan Wang
Institute of Cereal and Oil Crops, Hebei Academy of Agriculture and Forestry Sciences
Zhixiao Zhang
Institute of Cereal and Oil Crops, Hebei Academy of Agriculture and Forestry Sciences
Yingchao Shen
Institute of Cereal and Oil Crops, Hebei Academy of Agriculture Forestry Sciences
Jing Tian
Institute of Cereal and Oil Crops, Hebei Academy of Agriculture and Forestry Sciences
Baojie Fan
fanbaojie1972@163.com

Institute of Cereal and Oil Crops, Hebei Academy of Agriculture and Forestry Sciences
https://orcid.org/0009-0008-3675-9509

Research Article

Keywords: mung bean, herbicide tolerance, candidate gene, glutathione S-transferase U18

Posted Date: September 23rd, 2025

DOI: https://doi.org/10.21203/rs.3.rs-7555967/v1

License: This work is licensed under a Creative Commons Attribution 4.0 International License.
Read Full License

Version of Record: A version of this preprint was published at Theoretical and Applied Genetics on February 28th, 2026. See the published version at https://doi.org/10.1007/s00122-026-05184-y.

Abstract

Herbicides are widely applied for weed control in mung bean cultivation. Developing new varieties with herbicide resistance is critical for weed management in mung bean. In this study, a recombinant inbred line (RIL) population, developed from a cross between the fomesafen resistant variety LZ177 and the fomesafen susceptible variety LD235, was used to map the genes related to fomesafen herbicide resistance. The initial mapping performed with genetic mapping and BSA-seq revealed a candidate region of 1.17 Mb on chromosome 11. RNA-seq were performed using a residual heterozygous line 198 resistant (RHL198-R) and susceptible (RHL198-S) line at 0, 12, 24, 48, and 72 h after fomesafen treatment. Gene mapping, BSA-seq, and RNA-seq identified a total of 13 potential candidate genes, of which one-base (A) insertion/deletion in the exon of *jg37117*, which encode a tau class glutathione S-transferase U18 (GSTU18), was determined to be the most promising candidate gene. We detected an A deletion in the exon of *VrGSTU18* in the susceptible lines, which are more susceptible to fomesafen than those lacking this deletion. *VrGSTU18* was cloned from LZ177 and subsequently transferred into *Arabidopsis.* Compared with WT plants, the *VrGSTU18*-overexpressing T_1 transgenic seedlings were more resistant to fomesafen herbicide. This study identified candidate gene potentially conferring resistance to fomesafen herbicide, providing a theoretical foundation for future research in mung bean breeding.

Key message

Gene mapping, BSA-seq, and RNA-seq uncovered genes associated with fomesafen herbicide tolerance in Mung bean. The function of a candidate gene was further validated using *VrGSTU18*-overexpressing T_1 transgenic *Arabidopsis* seedlings.

Introduction

Mung bean (*Vigna radiata* L.), an important short life cycle legume crop, is cultivated mainly in South, East, and Southeast Asia (Kang et al. 2014; Schafleitner et al. 2015). This crop provides a source of easily digestible protein; contains important nutrients, particularly folate and iron; and has extensive medicinal functions (Nair et al. 2019). Mung bean also fixes nitrogen in the soil and increases the quality of crops grown in the field after the mung beans are harvested (Graham and Vance 2003).

Mung bean yield and quality are influenced mostly by weeds, insect pests, and causal organisms of diseases (Rana et al. 2016). Among these, weeds are becoming the most serious problem and require more scientific attention. Uncontrolled weeds have been reported to cause 20–90% yield losses in various legume crops (Pooniya et al. 2015; Rana et al. 2016). The development of herbicide-resistant crops has become a useful strategy for weed control, which can reduce the phytotoxicity of herbicides to crops and improve the chemical weeding efficiency (Green 2014). Traditional mutagenesis breeding, transgenic breeding, and CRISPR/Cas-based techniques are the primary methods used to develop herbicide-resistant crops (Dong et al. 2021).

Fomesafen, one of the diphenyl ether classes of protoporphyrinogen oxidase (PPO)-inhibitor herbicides, was used to control broadleaf weeds, grasses, and sedges in the cultivation of food legumes (Salas et al. 2016). In plants, chloroplastic PPO1 (encoded by *PPX1*) and mitochondrial PPO2 (encoded by *PPX2*), are the targets of PPO-inhibitor herbicides (Lermontova et al. 1997). PPO inhibitor herbicides prevent the conversion of protoporphyrinogen IX to protoporphyrin IX, causing an excessive accumulation of protoporphyrinogen IX, which leaks into the cytoplasm (Matringe et al. 1989).

Generally, there are two main types of herbicide resistance: target site resistance (TSR) and nontarget site resistance (NTSR). TSR involves mutations in a protein-coding region (reducing its interaction with herbicides) or occurs by overproduction of the target enzyme (Gaines et al. 2020; Sammons and Gaines 2014). The genes encoding acetolactate synthase (*ALS*), acetyl-CoA carboxylase (*ACCase*), 5-enolpyruvylshikimate-3-phosphate (*EPSPS*), and protoporphyrinogen IX oxidase (*PPO*) play critical roles in generating herbicide-resistant plants through TSR (Dong et al. 2021; Giacomini et al. 2017; Powles and Yu 2010). NTSR mechanisms primarily involve reduced herbicide absorption or translocation, as well as enhanced sequestration or metabolic degradation (Gaines et al. 2020; Jugulam and Shyam 2019). Several families of herbicide-degrading enzymes, including cytochrome P450 monooxygenases, glutathione *S*-transferases (GSTs), glucosyl transferases (GTs), and aryl acylamidases, have been identified and characterized (Gaines et al. 2020; Jugulam and Shyam 2019; Powles and Yu 2010; Yu and Powles 2014).

Breeding herbicide resistant mung bean varieties is an essential approach for controlling weed. Studies on gene localization and resistance mechanisms offer a theoretical foundation for resistance breeding. In this study, we selected a residual heterozygous line 198 (RHL198) with a heterozygosity interval of SSR2755 ~ SSR2951 on chromosome 11 from the RIL population. The F_2 population generated from self-pollinated RHL198 was subjected to transcriptome analysis to detect changes in the RHL198-R and RHL198-S lines after fomesafen treatment. Gene mapping, BSA-seq, and RNA-seq were performed to identify fomesafen resistance-associated genes. This study provides a strong foundation for further elucidating the resistance mechanisms in mung bean breeding.

Materials and methods

Plant materials and phenotypic identification

An RIL population with 302 individuals was developed from a cross of LZ177 and LD235 using a single-seed descent method. LZ177 is a germplasm resource obtained from Liaoning Province, China, which is highly resistant to the herbicide fomesafen, whereas LD235 originates from Hubei Province, China, and is highly susceptible to the herbicide fomesafen. The F_2 population generated by self-pollination of an RHL198 line selected in the F_7 generation with a heterozygous interval of SSR2755 ~ SSR2951 on chromosome 11 was used as the RNA-seq material.

Seeds were planted in plastic containers, and cultivated in a greenhouse maintained at 22–25°C with 60% relative humidity for 30 days. At the 2–3 trifoliate leaf stage, ten plants for each line with three replicates were treated with fomesafen using a precision laboratory sprayer calibrated to deliver 262.5 g ai ha^{-1} at the manufacturer's recommended application rate. Symptoms of damage were investigated on the 3rd day after treatment. With herbicide resistance treated as a qualitative trait, the classification follows the above grading system: Homozygous herbicide resistant is denoted as "A", homozygous herbicide susceptible as "B", and heterozygous herbicide-resistant as "H".

Construction of the genetic map and gene mapping

Total genomics DNA were extracted from the young leaves of each plant by CTAB method (Chen et al. 1999). A genetic linkage map was constructed using QTL IciMapping v4.0 (Meng et al. 2015). The QTLs were analyzed using the inclusive composite interval mapping of the additive (ICIM–ADD) method (Li et al. 2007). The LOD threshold of the 1000 permutations test value was set to 2.5 to determine the putative QTL.

BSA-seq

Total genomics DNA were extracted from young leaves and 30 extremely resistant (R) and susceptible (S) lines were selected on the basic of their damage symptoms. Genomic DNA was extracted from the parental lines and two pooled samples using the CTAB method (Chen et al. 1999). The qualified DNA library was subsequently sequenced on an MGI-2000 platform. The raw reads were quality-filtered and aligned to the “Jilv7” reference sequence (Liu et al. 2022). The GATK software tool was used to detect SNPs (McKenna et al. 2010). The SNP index was calculated by comparing the allele frequencies between the R and S bulks against the parental references. Statistical significance was determined through 1,000 permutation tests, with candidate regions identified at a 95% confidence threshold. The final candidate intervals were derived through the integration of Euclidean distance (ED) and SNP-index approaches.

RNA-seq

The RHL198-R and RHL198-S seedlings at 0, 12, 24, 48, and 72 h after treatment with fomesafen were subjected to RNA-seq analysis. Ten individual plants from RHL198-R and RHL198-S were sampled at five distinct time points with three replicates. A total of 30 RNA samples were processed with an RNAprep Pure Plant Kit (Tiangen, Beijing, China). Illumina sequencing was performed at Bmkgene (China). High-quality clean data were generated through filtering out adapter sequences and low-quality reads of the raw data. Reads were aligned to the “Jilv7” reference genome (http://njh.biobin.com.cn) with HISAT2 tools (Kim et al. 2015). Subsequently, the mapped reads were assembled using StringTie (Pertea et al. 2015). Differential expression analysis was conducted by DESeq2 (Subramanian et al. 2005).

GO enrichment analysis of the DEGs was conducted via the clusterProfiler package (Yu et al. 2012) based Wallenius noncentral hypergeometric distribution to account for gene length bias (Young et al. 2010). For pathway analysis, we assessed the statistical enrichment of DEGs in KEGG pathways using KOBAS in conjunction with clusterProfiler (Mao et al. 2005). Weighted gene co-expression network analysis (WGCNA) was performed using the BioCloud platform (https://www. biocl oud. net/). Gene modules were identified with the following parameters: soft-thresholding power β = 19 (Fig. S1) and a minimum module size of 30 genes.

Quantitative real-time PCR (qRT−PCR) analysis

RNA-seq findings were validated through qRT−PCR of selected candidate genes. First-strand cDNA was synthesized utilising the FastKing gDNA Dispelling RT−PCR System (Tiangen Biotech, Beijing, China). qRT−PCR was employed using 150 ng of cDNA, 10 μL of SuperReal PreMix Plus (Tiangen, Beijing, China) and 0.3 μM primer in a 20 μL volume. The relative expression of target genes was computed with the $2^{-\Delta\Delta CT}$ method (Schmittgen and Livak 2008). The experiments were performed via a Roche LightCycler, and the data were normalized relative to those of the housekeeping gene *CYP2* (Jian et al. 2008). The primers used here are listed in Table S1.

Construction of vectors and generation of transgenic Arabidopsis plants

The full-length CDS without a stop codon of *VrGSTU18* was subsequently cloned and inserted into the plant binary vector pSuper1300-GFP driven by the CaMV 35S promoter. The primers used here are listed in Table S1. The VrGSTU18-GFP construct was introduced into *Arabidopsis* (ecotype Columbia) via the floral dip method (Clough and Bent 1998).

Subcellular localization

To analyze the subcellular localization of GSTU18, roots from seven-day-old *Arabidopsis* seedlings of T_1 generation expressing VrGSTU18-GFP was used. The images were collected using a Leica laser confocal microscope (Leica, Germany).

Results

Genetic analysis of the fomesafen resistance gene

Germplasm LZ177 and LD235, which were collected from Liaoning and Hubei Provinces in China, respectively, showed different levels of resistance to fomesafen. The LZ177 strain was resistant to fomesafen, while the LD235 strain was susceptible to it. After fomesafen treatment, the LD235-treated plants exhibited leaf yellowing, plant wilt and death on the 3rd day. However, all LZ177 plants and their F_1 progeny seedlings remained healthy (Fig. 1a–c). The F_2 population exhibited resistance segregation. An investigation of segregation revealed that genetic segregation in the $F_{2:3}$ population (87 homozygously

resistant:158 heterozygous:95 homozygously susceptible) occurred at a 1:2:1 ratio ($\chi 2 = 2.07 < \chi 2_{0.05}=3.84$), indicating the single dominant gene inheritance of fomesafen resistance (Table 1).

Table 1
Reactions of LZ177, LD235 and their derived populations to fomesafen treatment

Sample	Total plants	Resistant	Segregating	Susceptible	Expected ratio	χ^2
LZ177	30	30	—	0		
LD235	30	0	—	30		
F_1	30	30	—	0		
$F_{2:3}$	340	87	158	95	1:2:1	2.07

Construction of the genetic map and gene mapping

The genetic linkage map was constructed with 133 polymorphic SSR markers from a total of 4,047 SSR markers (Liu et al. 2017) using RIL population comprising 302 individuals. The genetic map had a total length of 1108.13 centimorgans (cM). The length of the 11 linkage groups ranged from 4.17 cM (LG. 1) to 188.75 cM (LG. 3), with an average size of 100.74 cM (Fig. 2, and Table 2). Following the mapping approach for a dominant single gene, the herbicide resistance gene *HR1* was integrated as a phenotypic marker and analyzed together with 133 polymorphic markers for linkage analysis. The gene was mapped to linkage group LG11, which matched to chromosome 11, and was flanked by SSR2755 and SSR2951 with a physical interval from 20,427,755 ~ 21,595,065 bp. The genetic distances to the flanking markers were 3.05 cM and 1.78 cM, respectively (Fig. 2, and Table 3).

Table 2
Information on the genetic linkage map

Linkage group	Marker numbers	Length/cM	Average distance/cM
LG1	3	4.17	1.39
LG2	15	143.95	9.60
LG3	26	188.75	7.26
LG4	10	130.75	13.08
LG5	8	76.42	9.55
LG6	14	106.04	7.57
LG7	10	144.53	14.45
LG8	5	42.33	8.47
LG9	4	53.41	13.35
LG10	6	132.04	22.01
LG11	32	85.74	2.60
Total	133	1108.13	8.27

BSA-seq

To validate the identification the candidate regions, BSA-seq was carried out using 30 extremely resistant and susceptible individuals from the RIL population to construct resistant pool (RP) and susceptible pool (SP), respectively. The RP and SP, and the LZ177 and LD235 parental lines were subjected to Illumina high-throughput sequencing. More than 378 Mb of clean reads with Q30 ≥ 92.71% were obtained. With respect to the RP, SP, LZ177 and LD235, 98.53%, 98.36%, 98.53%, and 98.58% of the reads, respectively, could be mapped to the “Jilv7” reference genome, respectively (Table S2). ΔSNP-index and ED analyses of the RP and SP SNPs revealed the associated region. Four candidate regions on Chr. 11 (6.23–12.75 Mb, 16.65–17.97 Mb, 20.08–21.87 Mb, and 21.90-29.37 Mb) were identified as candidate intervals on the basis of significant linkage disequilibrium (Fig. 3, and Table 3). Combining the BSA-seq and linkage analysis results, a 1.17 Mb region on Chr11 was identified as the candidate interval.

Table 3
Information on the associated regions detected using different methods.

Associated analysis method	Chromosome	Start region (bp)	End region (bp)	Size (Mb)
SNP-index	Chr06	1	500,001	0.5
	Chr11	2,000,001	30,500,001	28.5
ED	Chr11	6,232,923	12,757,251	6.5
	Chr11	16,653,166	17,974,885	1.32
	Chr11	20,086,225	21,873,833	1.78
	Chr11	21,896,508	29,373,158	9.47
Linkage analysis	Chr11	20,427,755	21,595,065	1.17
Association results	Chr11	20,427,755	21,595,065	1.17

RNA-seq

To investigate genes that respond to fomesafen exposure, RNA-seq was performed using RHL198-R and RHL198-S plants treated with fomesafen for 0, 12, 24, 48, and 72 h. A total of 1,231,561,800 clean reads were obtained (6 Gb/sample), with Q20 (≥ 96.72%) and Q30 (≥ 91.53%) scores. Reads aligned to the reference genome at an average of 93.48% (88.11% unique) with 43.66% GC content (Table S3). We identified 6980 DEGs in RHL198-R at 12, 24, 48, and 72 h after fomesafen treatment compared with 0 h, and 16,159 DEGs were found in RHL198-S (Fig. 4 and Table S4). Combining the DEGs in RHL198-R and RHL198-S, 17,382 DEGs were associated with fomesafen resistance (Table S4), of which 5,757 DEGs were related to the response of fomesafen treatment in both lines (Fig. 4e).

To elucidate the candidate genes underlying fomesafen resistance, we conducted differential expression analyses between the R and S lines. A total of 574, 8487, 4576, 6635, and 11,610 DEGs were found between RHL198-R and RHL198-S at 0, 12, 24, 48, and 72 h, respectively (Table S5), with a total of 15,488 DEGs associated with resistance response, 9,267 of which were found in more than two groups (Fig. 4d).

Among the 15,488 resistance-associated DEGs and 17,382 fomesafen-responsive DEGs, 14,402 overlapping genes were identified (Fig. 4e). These 14,402 DEGs are differentially expressed in response to both herbicide treatment and resistance, indicating they may play roles in fomesafen resistance in mung bean.

These DEGs were significantly enriched in 5116 terms. The majority terms were “translation,” “photosynthesis,” “ribosome,” “chloroplast,” “structural constituent of ribosome,” and “oxidoreductase activity” (Fig. S2a). Moreover, these DEGs were assigned to 135 KEGG pathways. Most DEGs were enriched in “plant pathogen interaction” and “plant hormone signal transduction” (Fig. S2b). These results offer a reference for additional screening of fomesafen resistance-related genes in mung bean.

WGCNA

To validate the identification genes associated with herbicide resistance in mung bean, WGCNA was performed with 20,001 genes selected to build the network after low-expression genes (an average FPKM of < 1) were filtered out. Soft thresholding powers with β = 19 were selected for screening the network topology and performing an additional cluster dendrogram analysis. When the power value was 19, a total of 13,143 genes were classified into 17 modules with similar expression trends ranging from 80 to 2,597 genes, as indicated by distinct colors in the cluster dendrogram. The 980 unassigned genes were grouped into the grey module (Fig. 5a and Table S6). Module correlation analysis revealed highly associated gene clusters, potentially indicating their cooperative roles in biological processes (Fig. 5b).

Nine modules were significantly associated with fomesafen resistance ($p < 0.01$). Three modules showed positive correlations: maroon (2,214 genes), yellowgreen (953 genes), and darkorange2 (361 genes), suggesting their potential roles in enhancing herbicide resistance. Conversely, six modules exhibited negative correlations: brown (2,597 genes), blue2 (80 genes), thistle3 (549 genes), darkorange (891 genes), mediumpurple1 (538 genes), and antiquewhite4 (173 genes), indicating their negative regulation of resistance (Fig. 5c, and Table S6).

Identification and characterization of candidate genes

Through integrating BSA-seq, RNA-seq, and WGCNA data in the candidate regions based on the genetic map, 13 potential candidate genes were identified potentially involved in fomesafen resistance. Among these genes, nine genes were highly expressed in the resistant line, whereas seven genes showed higher expression in the susceptible line (Fig. 5d). Notably, three genes, *jg35117*, *jg35121*, and *jg35124*, which encode the tau class GSTU18, GSTU17-like (GSTU17L), and GSTU17, respectively, emerged as strong candidate genes, which is consistent with studies showing that GSTUs are primarily responsible for detoxifying photobleaching diphenyl ether herbicides (Dixon et al. 2003; Thom et al. 2002). While no SNP or InDel variations were detected in the exons of *VrGSTU17L* and *VrGSTU17*, we detected a single-nucleotide deletion (A) in the exon of *VrGSTU18* at the 189th position in the susceptible lines, which caused a frameshift mutation that introduced a premature stop codon (Fig. 6a). Moreover, qRT—PCR analysis revealed that *VrGSTU18* transcript level was significantly higher in resistant lines, which is consistent with the RNA-seq results (Fig. 6b). We also sequenced the *VrGSTU18* gene in some RIL and RHL198 populations, and the results showed that all the susceptible lines had an A deletion in the exon of *VrGSTU18*, whereas the resistant lines lacked this deletion (Fig. 6c). In conclusion, the *VrGSTU18* gene was identified as a strong candidate gene because susceptible lines carrying the mutated *VrGSTU18* gene cannot detoxify the herbicide.

Generation of transgenic Arabidopsis plants overexpressing VrGSTU18 and fomesafen resistance

To confirm these results, *VrGSTU18*-GFP constructs cloned from the LZ177 population were generated by fusing the full-length CDS to the binary vector pSuper1300-GFP, driven by the CaMV 35S promoter, and then transferred into *Arabidopsis*. Compared with the WT plants, the T_1-overexpressing *Arabidopsis* lines presented enhanced tolerance to 10μM fomesafen treatment (Fig. 6d), which indicates the efficient detoxification of fomesafen by *VrGSTU18-GFP* transgenic plants. Subcellular localization showed the T_1

transgenic *GSTU18-GFP Arabidopsis* was expressed in the cytoplasm (Fig. 6e), where is highly active in detoxifying fomesafen.

Discussion

Weeds significantly affect the yield and quality of mung bean. Herbicides are widely used for weed control in the field. The development of herbicide-resistant crops is an economical way to manage weeds. In the present study, two mung bean germplasms, LZ177 and LD235, presented opposite phenotypes after fomesafen treatment: all LZ177 plants were resistant to fomesafen treatment, while the LD235 strain was susceptible (Fig. 1), indicating that the fomesafen herbicide resistance is controlled as a qualitative trait, which is governed by a single dominant gene. The qualitative resistance phenotype makes it suitable for resistance gene screening by integrating BSA-seq and RNA-seq. In recent years, combining BSA-seq with RNA-seq has become an effective approach for fine-mapping genes, which can identify candidate genes quickly and excatly. For example, BSA-seq and RNA-seq analyses revealed candidate genes associated with visual stay-green (Zheng et al. 2023), inflorescence architecture and kernel orientation by phytohormone homeostasis in maize (Wang et al. 2023). Ye et al., (2022a, 2022b) applied a combined approach to identify not only identify candidate genes involved in plant architecture, but also four genes responsible for the albino phenotype in Brassica napus. Fang et al., (2025) developed F_2 population, conducted a genetic map and QTL mapping with 493 polymorphic markers, and combined RNA-seq analysis to identify two QTLs, *qOIL1.2* and *qPRO14.1* related to oil and protein in soybeans. In this study, we constructed a genetic map with 133 polymorphic markers, and integrated BSA-seq, RNA-seq, as well as WGCNA data, 13 candidate genes on chromosome 11 were likely responsible for fomesafen resistance (Fig. 5). Among these genes, *jg35117* (*VrGSTU18*), which encode the tau class GSTU18, is the strongest candidate gene, and there is an A deletion in an exon of *VrGSTU18* at position 189 that causes the frameshift mutations, resulting in the formation of a short protein. A premature stop mutation in the resulting *VrGSTU18* transcript might explain the observed fomesafen resistance.

GSTs are key enzymes involved in the detoxification of herbicides. Plant GST genes can be classified into four classes: Phi, Zeta, Tau, and Theta. Among them, the Phi and Tau classes are plant-specific and represent the largest groups, playing predominant roles in herbicide detoxification (Dixon et al. 2002, 2003; McGonigle et al. 2000). In particular, soybean has a high capacity for detoxifying diphenyl ether herbicides, such as fomesafen, via GST-mediated thiol conjugation (Andrews et al. 1997). Overexpression of the *GmGSTU4* isoenzyme in transgenic tobacco has been shown to increase its tolerance to both diphenyl ether and chloroacetanilide herbicides (Benekos et al. 2010). Similarly, the heterologous expression of *OsGSTU3* and *OsGSTU4* in *Escherichia coli* revealed their high catalytic activity toward chloroacetanilide herbicides (Jo et al. 2011; Lee et al. 2011). Transgenic *Arabidopsis* expressing the *A. myosuroides GSTF1* gene (*AmGSTF1*) has improved tolerance to some herbicides (Cummins et al. 2013). The expression of a maize GST gene in transgenic wheat confers herbicide tolerance (Milligan et al. 2001). Maize is tolerant to triazine herbicides because of its high GST activity, which can catalyze the conjugation of triazine to glutathione (Powles and Yu 2010). Furthermore, reports

have revealed that *GST* genes may play important roles in metabolic resistance to glufosinate (He et al. 2023; Lei et al. 2024). In this study, GSTU18 was determined to be the most promising candidate gene. T_1 transgenic *Arabidopsis* seedlings overexpressing *VrGSTU18* exhibited partial, but not complete, resistance to the herbicide fomesafen compared to the WT (Fig. 6), indicating that additional genes are involved in the detoxification process. GSTU18-GFP localize to cytoplasmic, where occurs catalysis by conjugation with glutathione (GSH) and the less toxic products can then be partially metabolized (Skipsey et al. 2005).

Additionally, this study identified several genes that are correlate with the resistance of mung bean to herbicide (Fig. 5d). *jg35079* encodes a member of the nitrate transporter 1 (NRT1) family, whose members are resistant to the herbicide chlorate in *Medicago truncatula* and *Arabidopsis* (Salehin et al. 2014; Tsay et al. 1993). *jg35126* encodes galactosyltransferase, which is a potent target for herbicide screening (Botté et al. 2005). These genes may also be involved in the detoxification process.

Previous studies have identified a single amino acid mutation in the *PPX1* gene (A212T) and five amino acid mutations in the *PPX2* gene (△G210, R98L, R128G/M, and G399A) that confer resistance to PPO-inhibiting herbicides (Bi et al. 2020; Carvalho-Moore et al. 2021; Giacomini et al. 2017; Rangani et al. 2019; Salas-Perez et al. 2017; Salas et al. 2016). In our study, we detected a substitution at position 210 (G210A) (Fig. S3); however, this substitution has been reported to confer little or no resistance (Powles and Yu 2010). Therefore, we concluded that the sequence variation in *PPX* is unlikely to be responsible for the herbicide tolerance observed in our study. In this study, we identified a mutation of *VrGSTU18* in the susceptible lines, which prevented the herbicide from being detoxified in the sensitive lines. The resistance function of *VrGSTU18* necessitates further research. This study lay the foundation for further investigations of herbicide resistance breeding and can aid in the development of strategies for resistant mung bean breeding.

Declarations

Conflict of interest

The authors declare that they have no conflict of interest.

Ethical approval

The authors declare that this research was performed and reported in accordance with ethical standards of scientific conduct.

Funding

This research was supported by the National Natural Science Foundation of China (32401885), China Agriculture Research System of MOF and MARA-Food Legumes (CARS-08), Hebei Seed Science and Technology Innovation Team of Coarse Cereals and Food Legumes (21326305D), Hebei Agriculture

Research System-Innovation Team of Coarse Cereals and Food Legume (HBCT2023050205), Innovation Special Project of Hebei Academy of Agriculture and Forestry Sciences (2022KJCXZX-LYS-17).

Author contributions

HYS, CYL and SW designed the study, performed the phenotyping, genotyping, data analysis, and gene cloning. YW, ZXZ, YCS contributed to phenotyping and genotyping. HYS, BJF, and JT wrote the manuscript. All authors read and approved of the manuscript.

Data availability

The data supporting the conclusions of this study are included in the article and the supplementary files.

References

1. Andrews CJ, Skipsey M, Townson JK, Morris C, Jepson I, Edwards R (1997) Glutathione transferase activities toward herbicides used selectively in soybean. Pestic Sci 51:213–222. https://doi.org/10.1002/(SICI)1096-9063(199710)51:2<213::AID-PS622>3.0.CO;2-L
2. Benekos K, Kissoudis C, Nianiou-Obeidat I, Labrou N, Madesis P, Kalamaki M, Makris A, Tsaftaris A (2010) Overexpression of a specific soybean GmGSTU4 isoenzyme improves diphenyl ether and chloroacetanilide herbicide tolerance of transgenic tobacco plants. J Biotechnol 150:195–201. https://doi.org/10.1016/j.jbiotec.2010.07.011
3. Bi B, Wang Q, Coleman JJ, Porri A, Peppers JM, Patel JD, Betz M, Lerchl J, McElroy JS (2020) A novel mutation A212T in chloroplast Protoporphyrinogen oxidase (*PPO1*) confers resistance to PPO inhibitor Oxadiazon in *Eleusine indica*. Pest Manag Sci 76:1786–1794. https://doi.org/10.1002/ps.5703
4. Botté C, Jeanneau C, Snajdrova L, Bastien O, Imberty A, Breton C, Maréchal E (2005) Molecular modeling and site-directed mutagenesis of plant chloroplast monogalactosyldiacylglycerol synthase reveal critical residues for activity. J Biol Chem 280:34691–34701. https://doi.org/10.1074/jbc.M505622200
5. Carvalho-Moore P, Rangani G, Heiser J, Findley D, Bowe SJ, Roma-Burgos N (2021) *PPO2* mutations in *Amaranthus palmeri*: implications on cross-resistance. Agriculture 11:760–772. https://doi.org/10.3390/agriculture11080760
6. Chen D, Ronald P (1999) A rapid DNA minipreparation method suitable for AFLP and other PCR applications. Plant Mol Biol Report 17:53–57. https://doi.org/10.1023/A:1007585532036
7. Clough SJ, Bent AF (1998) Floral dip: a simplified method for *Agrobacterium*-mediated transformation of *Arabidopsis thaliana*. Plant J 16:735–743. https://doi.org/10.1046/j.1365-313x.1998.00343.x

8. Cummins I, Wortley DJ, Sabbadin F et al (2013) Key role for a glutathione transferase in multiple-herbicide resistance in grass weeds. Proc Natl Acad Sci U S A 110:5812–5817. https://doi.org/10.1073/pnas.1221179110
9. Dixon DP, Davis BG, Edwards R (2002) Functional divergence in the glutathione transferase superfamily in plants. J Biol Chem 277:30859–30869. https://doi.org/10.1074/jbc.M202919200
10. Dixon DP, McEwen AG, Lapthorn AJ, Edwards R (2003) Forced evolution of a herbicide detoxifying glutathione transferase. J Biol Chem 278:23930–23935. https://doi.org/10.1074/jbc.M303620200
11. Dong H, Huang Y, Wang K (2021) The development of herbicide resistance crop plants using CRISPR/Cas9-mediated gene editing. Genes 12:912. https://doi.org/10.3390/genes12060912
12. Fang X, Liu J, Jiang A, et al (2025) QTL mapping and multi-omics identify candidate genes for protein and oil in soybean. Theor Appl Genet 138:115. https://doi.10.1007/s00122-025-04904-0
13. Gaines TA, Duke SO, Morran S, Rigon CAG, Tranel PJ, Küpper A, Dayan FE (2020) Mechanisms of evolved herbicide resistance. J Biol Chem 295:10307–10330. https://doi.org/10.1074/jbc.REV120.013572
14. Giacomini DA, Umphres AM, Nie H, Mueller TC, Steckel LE, Young BG, Scott RC, Tranel PJ (2017) Two new PPX2 mutations associated with resistance to PPO-inhibiting herbicides in *Amaranthus palmeri*. Pest Manag Sci 73:1559–1563. https://doi.org/10.1002/ps.4581
15. Graham PH, Vance CP (2003) Legumes: importance and constraints to greater use. Plant Physiol 131:872–877. https://doi.org/10.1104/pp.017004
16. Green JM (2014) Current state of herbicides in herbicide-resistant crops. Pest Manag Sci 70:1351–1357. https://doi.org/10.1002/ps.3727
17. He S, Liu M, Chen W, Bai D, Liao Y, Bai L, Pan L (2023) *Eleusine indica* cytochrome P450 and glutathione S-transferase are linked to high-level resistance to glufosinate. J Agric Food Chem 71:14243–14250. https://doi.org/10.1021/acs.jafc.3c04325
18. Jian B, Liu B, Bi Y, Hou W, Wu C, Han T (2008) Validation of internal control for gene expression study in soybean by quantitative real-time PCR. BMC Mol Biol 9:59–72. https://doi.org/10.1186/1471-2199-9-59
19. Jo HJ, Lee JJ, Kong KH (2011) A plant-specific tau class glutathione S-transferase from *Oryza sativa* with very high activity against 1-chloro-2,4-dinitrobenzene and chloroacetanilide herbicides. Pestic Biochem Physiol 101:265–269. https://doi.org/10.1016/j.pestbp.2011.10.005
20. Jugulam M, Shyam C (2019) Non-target-site resistance to herbicides: recent developments. Plants 8:417. https://doi.org/10.3390/plants8100417
21. Kang YJ, Kim SK, Kim MY et al (2014) Genome sequence of mungbean and insights into evolution within *Vigna* species. Nat Commun 5:5443. https://doi.org/10.1038/ncomms6443
22. Kim D, Langmead B, Salzberg SL (2015) HISAT: a fast spliced aligner with low memory requirements. Nat Methods 12:357–360. https://doi.org/10.1038/nmeth.3317

23. Lee JJ, Jo HJ, Kong KH (2011) A plant-specific tau class glutathione S-transferase from *Oryza sativa* having significant detoxification activity towards chloroacetanilide herbicides. Bull Korean Chem Soc 32:3756–3759. https://doi.org/10.5012/bkcs.2011.32.10.3756
24. Lei T, Feng T, Wang L, Yuan X, Wu L, Wu B, Du J, Li J, Ma H (2024) Metabolic resistance mechanism to glufosinate in *Eleusine indica*. Pestic Biochem Physiol 204:106083. https://doi.org/10.1016/j.pestbp.2024.106083
25. Lermontova I, Kruse E, Mock HP, Grimm B (1997) Cloning and characterization of a plastidal and a mitochondrial isoform of tobacco protoporphyrinogen IX oxidase. Proc Natl Acad Sci U S A 94:8895–8900. https://doi.org/10.1073/pnas.94.16.8895
26. Li H, Ribaut JM, Li Z, Wang J (2007) Inclusive composite interval mapping (ICIM) for digenic epistasis of quantitative traits in biparental populations. Theor Appl Genet 116:243–260. https://doi.org/10.1007/s00122-007-0663-5
27. Liu C, Wang Y, Peng J et al (2022) High-quality genome assembly and pan-genome studies facilitate genetic discovery in mung bean and its improvement. Plant Commun 3:100352. https://doi.org/10.1016/j.xplc.2022.100352
28. Liu C, Wu J, Wang L, Fan B, Cao Z, Su Q, Zhang Z, Wang Y, Tian J, Wang S (2017) Quantitative trait locus mapping under irrigated and drought treatments based on a novel genetic linkage map in mungbean (*Vigna radiata* L.). Theor Appl Genet 130:2375–2393. https://doi.org/10.1007/s00122-017-2965-6
29. Mao X, Cai T, Olyarchuk JG, Wei L (2005) Automated genome annotation and pathway identification using the KEGG Orthology (KO) as a controlled vocabulary. Bioinformatics 21:3787–3793. https://doi.org/10.1093/bioinformatics/bti430
30. Matringe M, Camadro J, Labbe P, Scalla R (1989) Protoporphyrinogen oxidase as a molecular target for diphenyl ether herbicides. Biochem J 260:231–235. https://doi.org/10.1042/bj2600231
31. McGonigle B, Keeler SJ, Lau SMC, Koeppe MK, O'Keefe DP (2000) A genomics approach to the comprehensive analysis of the glutathione S-transferase gene family in soybean and maize. Plant Physiol 124:1105–1120. https://doi.org/10.1104/pp.124.3.1105
32. McKenna A, Hanna M, Banks E, Sivachenko A, Cibulskis K, Kernytsky A, Garimella K, Altshuler D, Gabriel S, Daly M, DePristo MA (2010) The genome analysis toolkit: a MapReduce framework for analyzing next-generation DNA sequencing data. Genome Res 20:1297–1303. https://doi.org/10.1101/gr.107524.110
33. Meng L, Li H, Zhang L, Wang J (2015) QTL IciMapping: integrated software for genetic linkage map construction and quantitative trait locus mapping in biparental populations. Crop J 3:269–283. https://doi.org/10.1016/j.cj.2015.01.001
34. Milligan AS, Daly A, Parry MAJ, Lazzeri PA, Jepson I (2001) The expression of a maize glutathione S-transferase gene in transgenic wheat confers herbicide tolerance, both in planta and in vitro. Mol Breed 7:301–315. https://doi.org/10.1023/A:1011652821765

35. Nair RM, Pandey AK, War AR et al (2019) Biotic and abiotic constraints in mungbean production—progress in genetic improvement. Front Plant Sci 10:1340. https://doi.org/10.3389/fpls.2019.01340
36. Pertea M, Pertea GM, Antonescu CM, Chang TC, Mendell JT, Salzberg SL (2015) StringTie enables improved reconstruction of a transcriptome from RNA-seq reads. Nat Biotechnol 33:290–295. https://doi.org/10.1038/nbt.3122
37. Pooniya V, Choudhary AK, Dass A, Bana RS, Rana KS, Rana DS, Tyagi VK, Puniya MM (2015) Improved crop management practices for sustainable pulse production: an Indian perspective. Indian J Agric Sci 85:747–758. https://doi.org/10.56093/ijas.v85i6.49184
38. Powles SB, Yu Q (2010) Evolution in action: plants resistant to herbicides. Annu Rev Plant Biol 61:317–347. https://doi.org/10.1146/annurev-arplant-042809-112119
39. Rana DS, Dass A, Rajanna G, Kaur R (2016) Biotic and abiotic stress management in pulses. Indian J Agron 61:S238–S248
40. Rangani G, Salas-Perez RA, Aponte RA, Knapp M, Craig IR, Mietzner T, Langaro AC, Noguera MM, Porri A, Roma-Burgos N (2019) A novel single-site mutation in the catalytic domain of protoporphyrinogen oxidase IX (PPO) confers resistance to PPO-inhibiting herbicides. Front Plant Sci 10:568. https://doi.org/10.3389/fpls.2019.00568
41. Salas-Perez RA, Burgos NR, Rangani G, Singh S, Refatti JP, Piveta L, Tranel PJ, Mauromoustakos A, Scott RC (2017) Frequency of Gly-210 deletion mutation among protoporphyrinogen oxidase inhibitor–resistant Palmer Amaranth (*Amaranthus palmeri*) populations. Weed Sci 65:718–731. https://doi.org/10.1017/wsc.2017.41
42. Salas RA, Burgos NR, Tranel PJ, Singh S, Glasgow L, Scott RC, Nichols RL (2016) Resistance to PPO-inhibiting herbicide in Palmer amaranth from Arkansas. Pest Manag Sci 72:864–869. https://doi.org/10.1002/ps.4241
43. Salehin M, Huang YS, Bagchi R, Sherrier DJ, Dickstein R (2014) Allelic differences in *Medicago truncatula* NIP/LATD mutants correlate with their encoded proteins' transport activities in planta. Plant Signal Behav 8:e22813. https://doi.org/10.4161/psb.22813
44. Sammons RD, Gaines TA (2014) Glyphosate resistance: state of knowledge. Pest Manag Sci 70:1367–1377. https://doi.org/10.1002/ps.3743
45. Schafleitner R, Nair RM, Rathore A, Wang YW, Lin CY, Chu SH, Lin PY, Chang JC, Ebert AW (2015) The AVRDC – The world vegetable center mungbean (*Vigna radiata*) core and mini core collections. BMC Genom 16:344–354. https://doi.org/10.1186/s12864-015-1556-7
46. Schmittgen TD, Livak KJ (2008) Analyzing real-time PCR data by the comparative CT method. Nat Protoc 3:1101–1108. https://doi.org/10.1038/nprot.2008.73
47. Skipsey M, Cummins I, Andrews CJ, Jepson I, Edwards R (2005) Manipulation of plant tolerance to herbicides through co-ordinated metabolic engineering of a detoxifying glutathione transferase and thiol cosubstrate. Plant Biotechnol J 3:409–420. https://doi.org/10.1111/j.1467-7652.2005.00134.x
48. Subramanian A, Tamayo P, Mootha VK, Mukherjee S, Ebert BL, Gillette MA, Paulovich A, Pomeroy SL, Golub TR, Lander ES, Mesirov JP (2005) Gene set enrichment analysis: a knowledge-based

approach for interpreting genome-wide expression profiles. Proc Natl Acad Sci U S A 102:15545–15550. https://doi.org/10.1073/pnas.0506580102

49. Thom R, Cummins I, Dixon DP, Edwards R, Cole DJ, Lapthorn AJ (2002) Structure of a tau class glutathione S-transferase from wheat active in herbicide detoxification. Biochemistry 41:7008–7020. https://doi.org/10.1021/bi015964x
50. Tsay Y, Schroeder J, Feldmann K, Crawford N (1993) The herbicide sensitivity gene CHL1 of *Arabidopsis* encodes a nitrate-inducible nitrate transporter. Cell 72:705–713. https://doi.org/10.1016/0092-8674(93)90399-B
51. Wang Y, Li Y, Zhang W et al (2023) BSA-Seq and transcriptomic analysis provide candidate genes associated with inflorescence architecture and kernel orientation by phytohormone homeostasis in maize. Int J Mol Sci 24:10728. https://doi.org/10.3390/ijms241310728
52. Ye S, Yan L, Ma X et al (2022a) Combined BSA-seq based mapping and RNA-seq profiling reveal candidate genes associated with plant architecture in *Brassica napus*. Int J Mol Sci 23:2472–2486. https://doi.org/10.3390/ijms23052472
53. Ye S, Yang J, Huang Y, Liu J, Ma X, Zhao L, Ma C, Tu J, Shen J, Fu T, Wen J (2022b) Bulk segregant analysis-sequencing and RNA-Seq analyses reveal candidate genes associated with albino phenotype in *Brassica napus*. Front Plant Sci 13:994616. https://doi.org/10.3389/fpls.2022.994616
54. Young MD, Wakefield MJ, Smyth GK, Oshlack A (2010) Gene ontology analysis for RNA-seq: accounting for selection bias. Genome Biol 11:R14. https://doi.org/10.1186/gb-2010-11-2-r14
55. Yu G, Wang LG, Han Y, He QY (2012) clusterProfiler: an R package for comparing biological themes among gene clusters. OMICS J Integr Biol 16:284–287. https://doi.org/10.1089/omi.2011.0118
56. Yu Q, Powles S (2014) Metabolism-based herbicide resistance and cross-resistance in crop weeds: a threat to herbicide sustainability and global crop production. Plant Physiol 166:1106–1118. https://doi.org/10.1104/pp.114.242750
57. Zheng R, Deng M, Lv D, Tong B, Liu Y, Luo H (2023) Combined BSA-seq and RNA-seq reveal genes associated with the visual stay-green of maize (*Zea mays* L.). Int J Mol Sci 24:1182–1199. https://doi.org/10.3390/ijms242417617

Figures

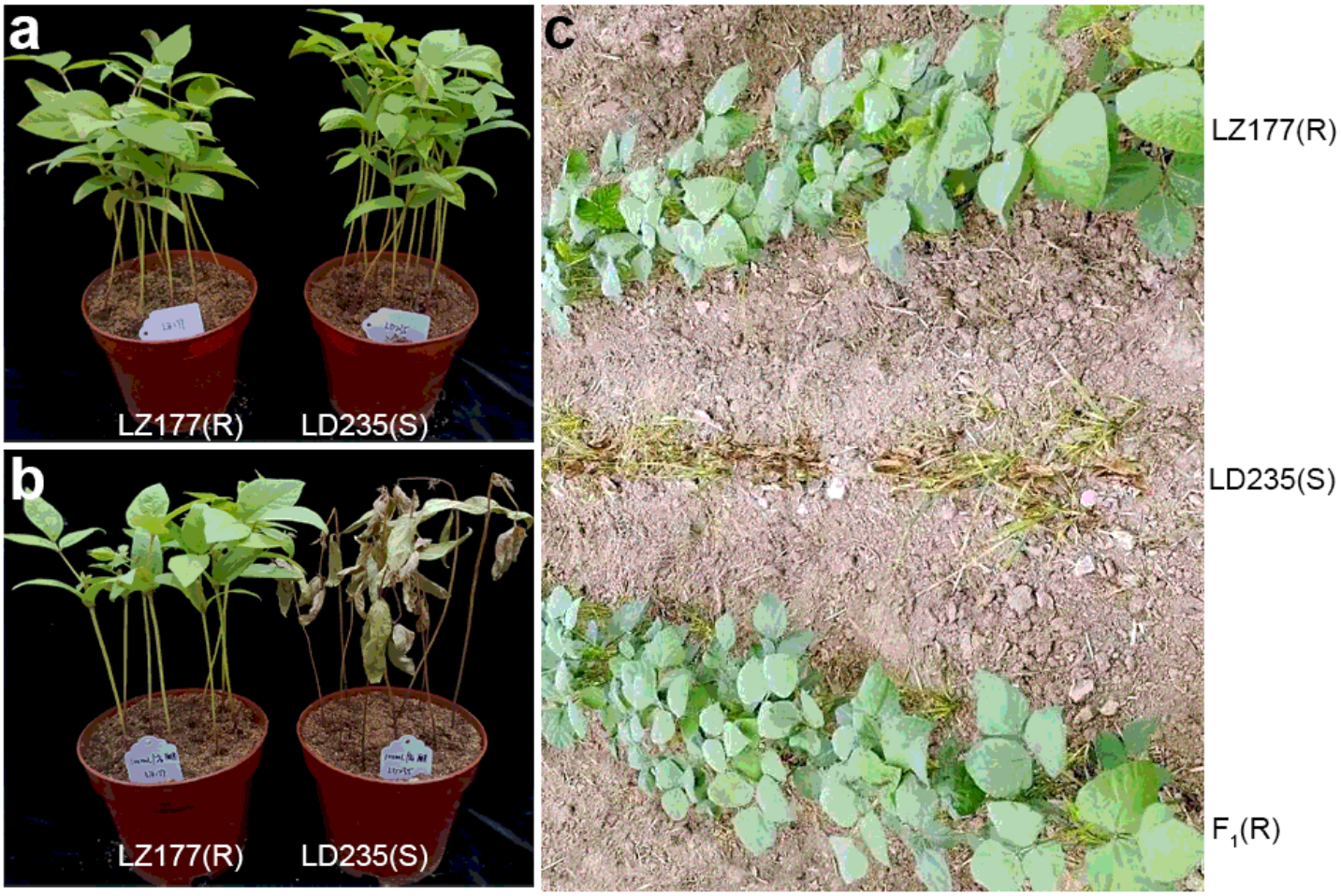


Figure 1

Symptoms of spraying with fomesafen in the resistant line (LZ177), the susceptible line (LD235), and their F_1 offspring. (a) The phenotype of the two lines at 0 h. Symptoms of spraying with fomesafen at 3 days in the parents (b) and their F_1 offspring (c)

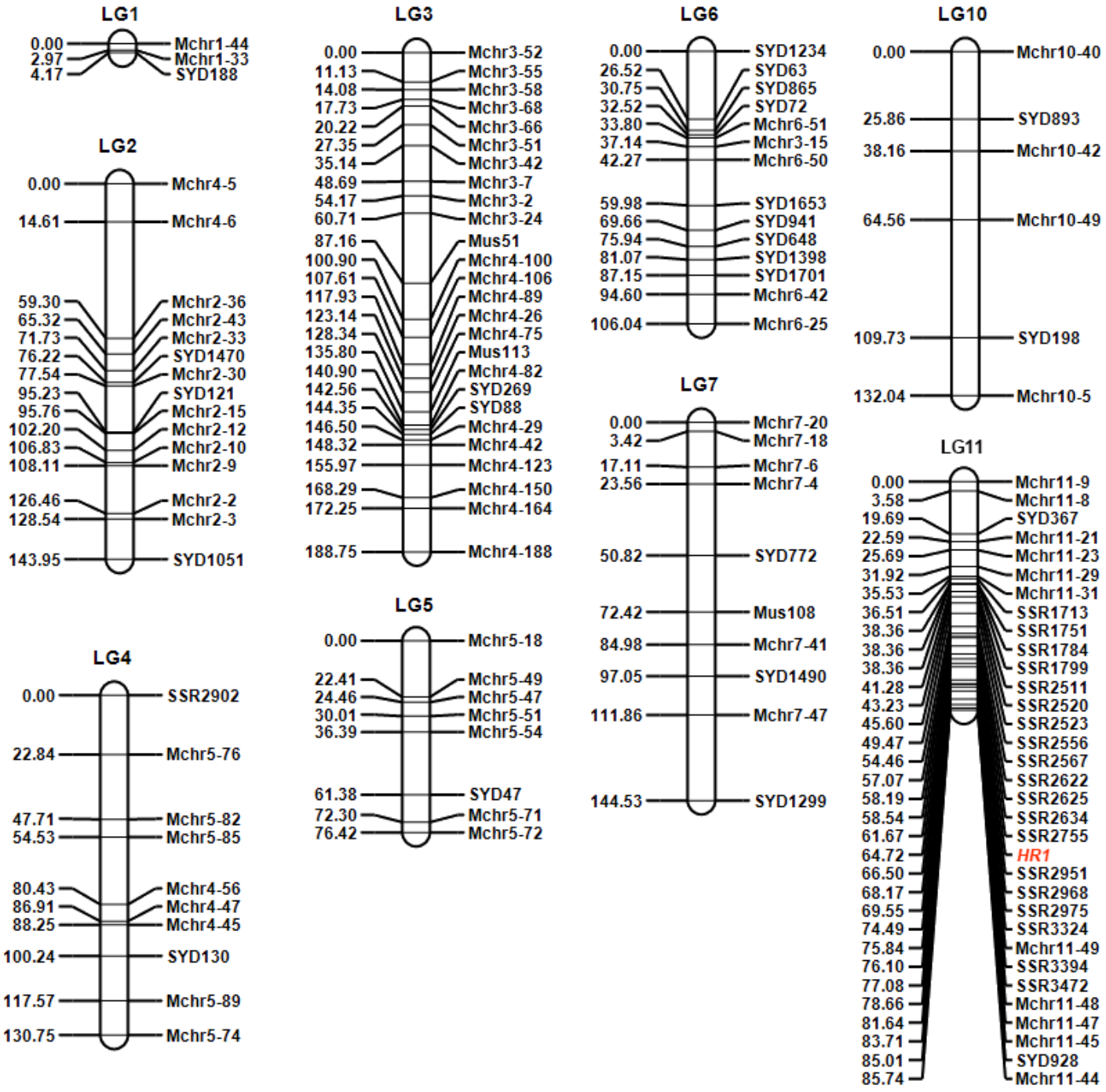


Figure 2

Construction of genetic linkage map based on SSR markers. Map distances and marker names are shown on the left and right sides of the linkage groups, respectively

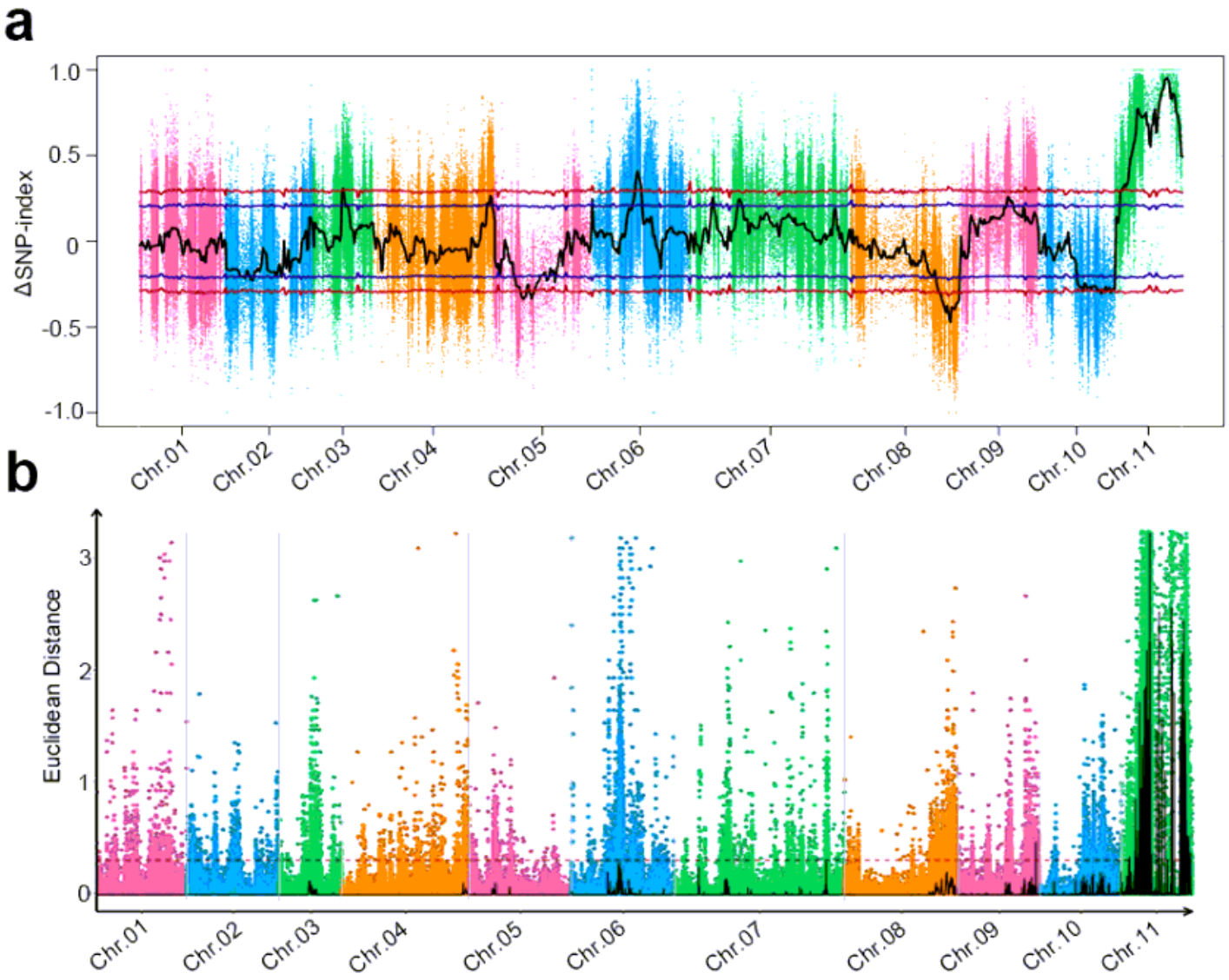


Figure 3

Identification of fomesafen resistance gene candidate intervals using two association methods. (**a**) Results of SNP correlation. (**b**) Results of ED correlation

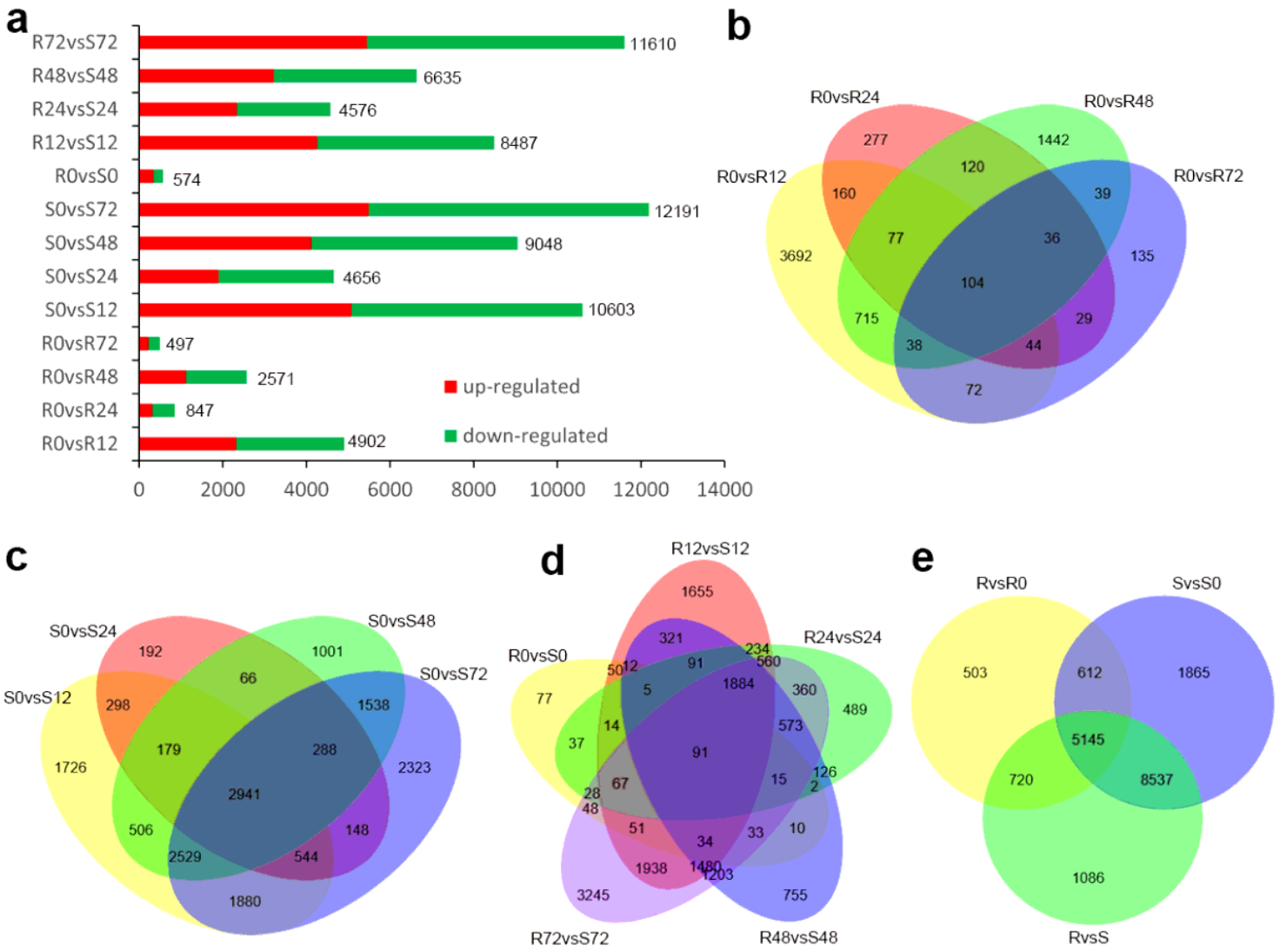


Figure 4

Differential expression analysis of RHL198-R and RHL198-S. (a) Number of DEGs in each pair. (b, and c) Venn diagram of the DEGs before and after fomesafen treatment in the R (b) and S (c) lines. (d) Venn diagram of the DEGs between the R and S lines. (e) Venn diagram of the DEGs in the two DEG analyses. R, resistant line RHL198-R; S, susceptible line RHL198-S; 0, 12, 24, 48, and 72 h after fomesafen treatment.

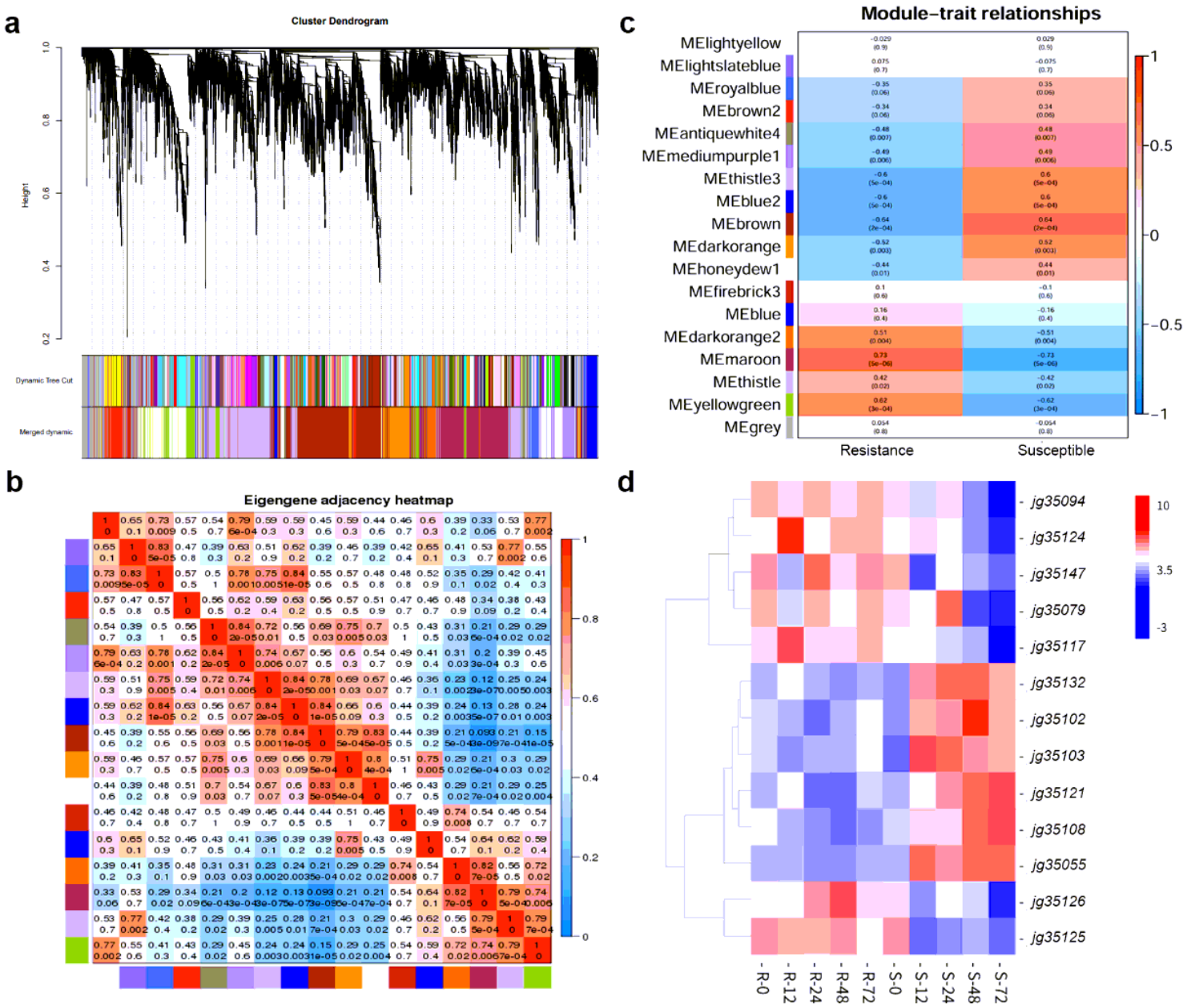


Figure 5

WGCNA of mung bean after spraying with fomesafen. (a) Cluster dendrogram of coexpression modules. (**b**) The heatmap showing the correlation coefficient between the modules. (**c**) Module–trait relationships. (d) Expression patterns of 13 candidate genes

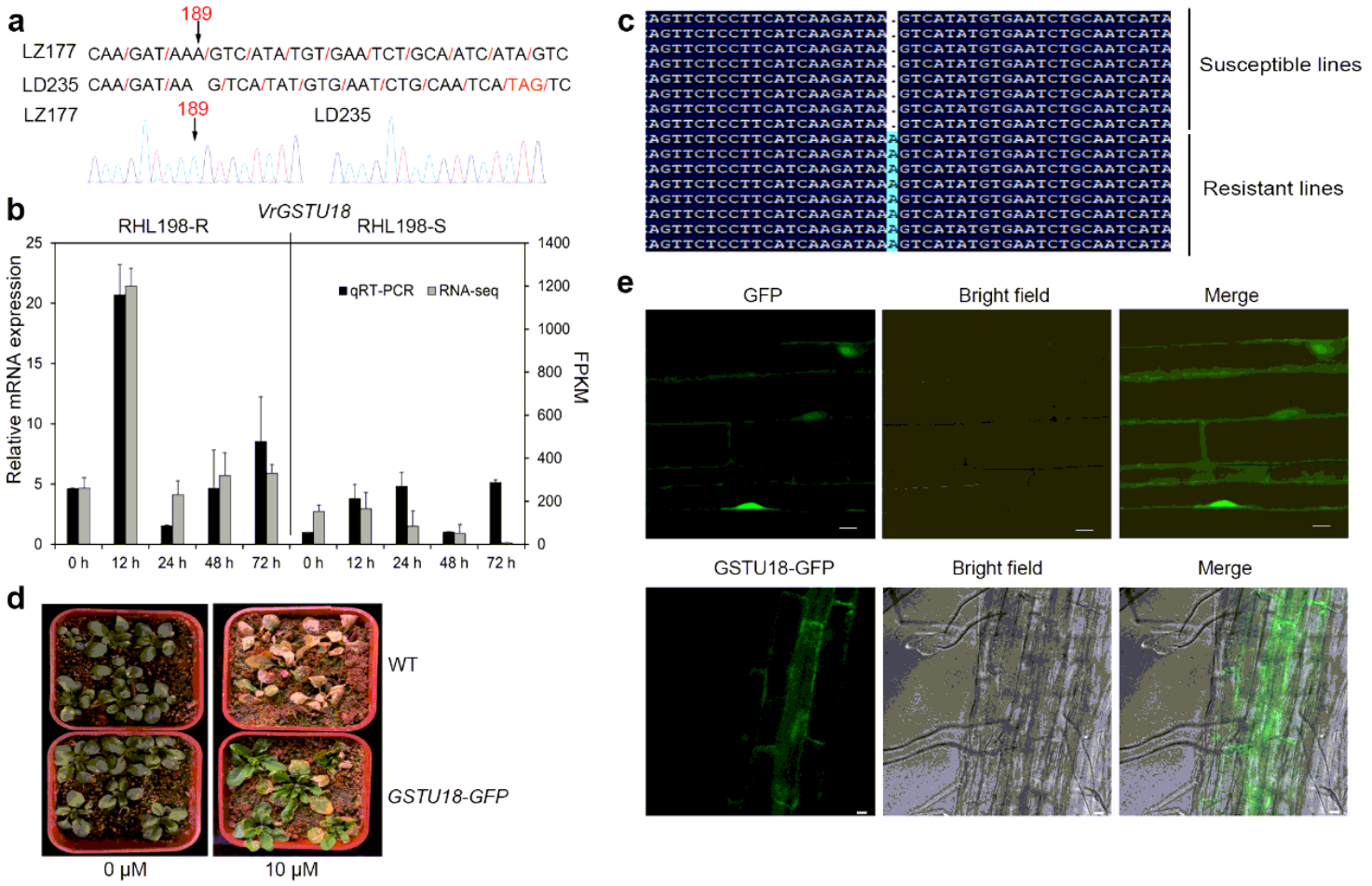


Figure 6

Validation of candidate genes. (a) Sequence alignment of *VrGSTU18* in LZ177 and LD235. (b) qRT–PCR validation of *VrGSTU18* in mung bean. RHL198-R, resistant line; RHL198-S, susceptible line; h, after treatment. (c) Sequence alignment of *VrGSTU18* in the susceptible and resistant lines in RIL and RHL198 populations. (d) Symptoms of spraying with 10 μM fomesafen at the 3rd day in three-week-old WT and *VrGSTU18-GFP* T_1 transgenic plants in *Arabidopsis*. (e) Subcellular localization of VrGSTU18 in T_1 transgenic *Arabidopsis* plants

Supplementary Files

This is a list of supplementary files associated with this preprint. Click to download.

- supplementaryfigures.docx
- supplementarytables.xlsx